HHS Public Access

Author manuscript

Nanotechnology. Author manuscript; available in PMC 2016 September 16.

Published in final edited form as:

Nanotechnology. 2013 March 29; 24(12): 125101. doi:10.1088/0957-4484/24/12/125101.

The effect of cryoprotection on the use of PLGA encapsulated iron oxide nanoparticles for magnetic cell labeling

Kevin S. Tang[a] and **Erik M. Shapiro**[a,b,*]

[a]Department of Biomedical Engineering, Yale University, New Haven, CT 06511, USA

[b]Molecular and Cellular MRI Laboratory, Magnetic Resonance Research Center, Department of Diagnostic Radiology, 300 Cedar Street, Yale University School of Medicine, New Haven, CT 06510, USA

Abstract

Magnetic PLGA nanoparticles are a significant advancement in the quest to translate MRI-based cell tracking to the clinic. The benefits of these types of particles are that they encapsulate large amounts of iron oxide nanocrystals within an FDA-approved polymer matrix, combining the best aspects of inert micron-sized iron oxide particles, or MPIOs, and biodegradable small particles of iron oxide, or SPIOs. Practically, PLGA nanoparticle fabrication and storage requires some form of cryoprotectant to both protect the particle during freeze drying and to promote resuspension. While this is a commonly employed procedure in the fabrication of drug loaded PLGA nanoparticles, it has yet to be investigated for magnetic particles and what effect this might have on internalization of magnetic particles. As such, in this study, magnetic PLGA nanoparticles were fabricated with various concentrations of two common cryoprotectants, dextrose and sucrose, and analyzed for their ability to magnetically label cells. It was found that cryoprotection with either sugar significantly enhanced the ability to resuspend nanoparticles without aggregation. Magnetic cell labeling was impacted by sugar concentration, with higher sugar concentrations used during freeze drying more significantly reducing magnetic cell labeling than lower concentrations. These studies suggest that cryoprotection with 1% dextrose is an optimal compromise that preserves monodispersity following resuspension and high magnetic cell labeling.

Introduction

Magnetic cell labeling is the fundamental principle behind MRI-based cell tracking. The use of superparamagnetic iron oxide nanoparticles as a magnetic cell label for this field has been well documented [1], and ample applications using MRI to specifically detect magnetically labeled cells have been demonstrated in both rodents and humans in numerous paradigms.

We have previously described the design, fabrication, and characterization of poly(D,L-lactide-co-glycolide) (PLGA) encapsulated iron oxide nanoparticles (NPs) dedicated for magnetic cell labeling [2]. PLGA NPs have been extensively used in the pharmaceutical field for drug delivery, however, they are limited by physical instability (aggregation/particle

*Corresponding author: Erik M. Shapiro, PhD, Department of Radiology, Michigan State University, 846 Service Rd, East Lansing, MI 48824, *Tel:* +1 (517)884-3270; *Fax:* +1 (517) 432-2849, erik.shapiro@rad.msu.edu.

fusion) and chemical instability (drug leakage of NPs) of the aqueous suspension for extended periods [3]. Freeze drying, or lyophilization, of NPs improves long term stability, but also exacerbates aggregation and nanoparticle fusion [4]. The addition of cryoprotectants to the freeze drying process has been shown to prevent NP aggregation and preserve initial NP formulation characteristics [5].

The use of cryoprotectants during the fabrication of PLGA encapsulated iron oxide NPs has never been investigated and thus, it is unknown what effect cryoprotection may have on magnetic cell labeling. We hypothesized that the addition of cryoprotectants would reduce particle aggregation upon suspension of particles in aqueous media, however it was difficult to predict how this might affect magnetic cell labeling. Therefore, we further sought to investigate the consequences of cryoprotection of PLGA encapsulated iron oxide particles on magnetic cell labeling.

Materials and Methods

Preparation of magnetic PLGA nanoparticles

Magnetite nanocrystals were synthesized according to Park, et al [6]. PLGA encapsulated magnetic nanoparticles (NPs) were fabricated as described in Nkansah, et al [2]. Briefly, 100 mg of magnetite nanocrystals and 100 mg of PLGA (I.V. ~0.67 dL/g, Mw ~40–75 kDa; Durect® Absorbables) was suspended in 2 ml methylene chloride (Sigma). The initial organic phase was added dropwise to 4 ml of 5% (w/v) PVA while vortexing, dispersed using a sonicator probe (Sonicator 350 cell disruptor) at 40% amplitude, and added to 60 ml of 0.3% (w/v) PVA and allowed to stir for 3 hours. PLGA encapsulated iron oxide NPs were isolated by centrifugation at 12,000 rpm for 10 minutes and washed thrice with dH_2O.

Cryoprotection and freeze drying of nanoparticles

PLGA encapsulated iron oxide NPs were fabricated as a single batch until the final cryoprotection step. Particles were divided into several groups and were freeze dried in the presence of various concentrations of either one of two different cryoprotectants, sucrose and dextrose, to investigate the influence of type and amount of cryoprotectant on freeze dried NP aggregation. Sucrose was used at 1%, 2%, and 5% (w/v) concentrations; dextrose was used at 0.01%, 0.1%, 1%, 2%, 5%, and 10% concentrations. Cryoprotectant percentages were partially chosen based on previous reports [4], and also based on our objective to pinpoint the concentration at which the ability of a cryoprotectant to act as a redispersant is compromised. According to Chacon et al, the presence of at least 5% cryoprotectant is essential to maintain the initial particle size [7].

Characterization of magnetic PLGA nanoparticles and cryoprotection effects

Nanoparticle morphology was analyzed via scanning electron microscopy (SEM) (FEI XL-30, ESEM-FEG). The particle size was determined by using ImageJ software to analyze particle areas from representative SEM images and calculating the diameter from the formula for area of a circle: $d=2\sqrt{A/\pi}$. The aggregation and polydispersity of particles were characterized using dynamic light scattering (ALV-5000 DLS). Data were collected in intervals of 30 s for all samples continuously over 15 min for a total of 30 measurements/

sample. On-board correlator cards provided the scattered light intensity correlation functions g(τ), which were fit to a second-order exponential decay function to obtain average particle sizes (cumulant analysis). The average particle size of each sample was obtained 30 times and the mean value was calculated and used to determine the ratio of initial particle size (S_i) and particle size after freeze drying (S_f). CONTIN analysis was used to obtain the particle size distributions [8]. Total iron content of the particles was determined by thermogravimetric analysis (TGA) (TA Instruments Q50 model). Lyophilized samples of nanoparticles were placed in aluminum dish and heated from 30 to 600°C at 10°C/min under the flow of nitrogen gas.

In vitro magnetic cell labeling

Mouse embryonic fibroblasts (STOs) were cultured in DMEM containing 10% fetal bovine serum, 1% L-glutamine, and 1% penicillin/streptomycin at 37°C under 5% CO_2. For labeling, cells were incubated with the same media containing PLGA encapsulated iron oxide NPs at ~300 μg/ml of iron for 24 hrs (Table 1). A commercially available iron oxide microparticle 1.63μm in diameter from Bangs Laboratories was also used as a benchmark. After labeling, cells were washed 3x with PBS to remove free NPs and digested in 36.5 % hydrochloric acid (Sigma). The iron content of each sample was determined using inductively coupled plasma–optical emission spectroscopy (Perkin-Elmer, Optima ICP-OES).

Results

Characterization of magnetic PLGA nanoparticles

SEM images of PLGA encapsulated iron oxide NPs without cryoprotection show discrete nanoparticles with highly spherical morphology consistent with previous preparations (Figure 1a–c) [2]. SEM micrographs of NPs with different cryoprotection schemes show spherical particles immobilized in matrices of sugar (Figure 1d–f). Analysis of SEM images of noncryoprotected NPs revealed a normal size distribution with an average diameter of 138 ± 35 nm (Figure 2).

Total magnetite content was determined using TGA. The thermograms for 3 samples are shown in Figure 3. The top graph plots the % weight as a function of temperature and shows the total percentage of PLGA polymer (and sugar if present) in the sample; the remaining weight at 600 °C is the magnetite. The bottom graph plots the magnitude of the weight % derivative as a function of temperature and highlights the temperature at which the PLGA polymer burns off. In the cryoprotected samples, there is an additional peak at ~200 °C highlighting the temperature at which the sugar burns off. The noncryoprotected particles consisted of 55.77% PLGA polymer and 44.23% magnetite. The encapsulation efficiency of iron was calculated using the following formula:

$$\frac{\text{Assayed } m_{Fe_3O_4} \text{ in sample } (wt\%)}{\text{Theoretical maximum } m_{Fe_3O_4} \text{ in sample } (wt\%)} \times 100\%$$

For the noncryoprotected particles, the encapsulation efficiency was 88.5% (44.23/50). Because the batch of particles was mixed together before freeze drying with and without cryoprotectant, the encapsulation efficiency of the cryoprotected particles is identical to that of the noncryoprotected particles. The decreased weight percentage of magnetite in the cryoprotected thermograms was due to the additional sugar weight. The magnetite percentages obtained through TGA for each particle sample were necessary for ensuring iron doses were consistent across each cryoprotectant type and percentage for the magnetic labeling experiments later.

Effects of cryoprotectant type and concentration on particle size

To determine whether cryoprotectant type and concentration had an effect on redispersion of our PLGA encapsulated iron oxide NPs, DLS measurements were made on aqueous suspensions of NPs after freeze drying with two common cryoprotectants (sucrose and dextrose) at different concentrations and compared with that of noncryoprotected NPs (Figure 4). There was little difference in size between the NPs obtained following sucrose and dextrose cryoprotection. However, the average size for noncryoprotected NPs was 1.4 fold larger than both the sucrose and dextrose cryoprotected NPs. Not surprisingly, the average size for cryoprotected NPs measured by DLS was nearly 2 fold larger than the size measured by SEM. This is because DLS measures hydrodynamic radius calculated from the diffusional properties of the particle, which includes both solvent (hydro) and shape (dynamic) effects [9]. The SEM measurement is performed on a 2D image of dry particles.

Aggregation of PLGA encapsulated iron oxide NPs occurs in culture during cell labeling and this phenomenon has been quantified using DLS. The addition of cryoprotectant resulted in smaller average sizes, a finding attributed to the ability of sugar additive to form a glassy amorphous matrix around the particles, preventing the particles from sticking together during removal of water [10]. The inconsequential size differences between dextrose and sucrose as cryoprotectants at equal concentrations implied that for the purpose of reducing particle aggregation for cell labeling, dextrose and sucrose worked equally well. Our results suggest that cryoprotecting with 1% dextrose preserves sizes just as well as cryoprotecting with 10% dextrose. Therefore, it was hypothesized that the cryoprotectant saturation point at which particle aggregation begins to occur is lower than 1% cryoprotectant. Because dextrose and sucrose produced similar NP sizes, only dextrose was used to determine the cryoprotectant saturation point for redispersion.

Minimum cryoprotectant percentage for redispersion

Figure 5 shows SEM micrographs comparing different batches of PLGA encapsulated iron oxide NPs without cryoprotectant and with increasing amounts of dextrose from 0.01% to 5%. The sugar matrix is not visible at the lower dextrose concentrations (0.01–0,1%). At 1% dextrose, particles became less delineated and at 2% dextrose, the sugar matrix is fully visible. The effects of cryoprotection were clearly visible under optical microscopy upon reconstitution of each particle type in DI water (Figure 6). Without cryoprotection (DI), particles exhibited significant aggregation which subsided with increasing amounts of cryoprotectant used during fabrication. Addition of cryoprotectant (0.01% D, 0.1% D)

slightly reduced the clumping, but large aggregates of particles were still visible. Only at 1% D and higher concentrations did the particles become more monodisperse.

Figure 7 shows comparison charts of average particle sizes determined by DLS before and after freeze drying and with and without cryoprotection. The first chart compares absolute size values; the second chart compares relative size ratios of particle size after freeze drying and initial particle size, S_f/S_i. Without cryoprotection, the difference in final to initial size is over two fold. Samples 1% and 2% dextrose most closely retained their initial characteristics on reconstitution with S_f/S_i ratios of 1.08 and 1.09 respectively. As dextrose percentages decrease below 1%, there was a substantial increase in measured size, indicating an increase in particle aggregation. Furthermore, the increased variability for the noncryoprotected NPs also reflected the increased aggregation. These results suggest the minimum cryoprotectant percentage for redispersion of PLGA encapsulated iron oxide NPs to be 1% for dextrose.

Particle size distributions

To investigate the polydispersity of the NP suspensions as the cryoprotectant % changed, we also performed a CONTIN analysis of the raw DLS data. Figure 8 shows the particle size distributions generated by CONTIN. The size distribution profiles of 1% and 2% dextrose (green and purple lines) match closely with that of the particles before freeze drying (orange line), consistent with the results in Figure 7. As cryoprotectant % decreases, there is a concomitant increase in particle size (0.1% D and 0.01% D). Furthermore, the average size increase with decreasing amounts of cryoprotectant is accompanied by an increase in polydispersity of the particles in suspensions. Increased polydispersity is a strong indicator of increased particle aggregation, and was expected to be the highest in the noncryoprotected sample. Thus, in analyzing particle size, S_f/S_i ratio, and polydispersity, we concluded the minimum cryoprotectant percentage for retaining initial physical characteristics of our magnetic PLGA NPs was 1% dextrose.

In vitro magnetic cell labeling

To determine the effect of cryoprotectant on magnetic cell labeling, STO fibroblasts were labeled with noncryoprotected and various cryoprotected NPs for 24 hours. Before analyzing the iron content in each sample using ICP-OES, optical microscope images were acquired of the labeled fibroblasts to visualize the effects of the different cryoprotectants on particle aggregation (Figure 9). Large clumping was observed in the cells labeled with noncryoprotected NPs (DI). Very little clumping was observed in fibroblasts labeled with 2% dextrose NPs and almost no clumping observed in 5% sucrose and dextrose NP labeled fibroblasts.

ICP-OES was performed to determine total intracellular iron content in each sample. The iron content was then normalized to the total number of cells in each sample and a measure of iron weight/cell number obtained. Table 2 summarizes the results of the magnetic cell labeling experiment. Labeling efficiency is the amount of intracellular iron/sample over the initial iron amount added for labeling. Noncryoprotected particles had the highest label yield with ~40 pg iron/cell and therefore the highest iron labeling efficiency (~20%). The addition of cryoprotectant to the NP caused the labeling efficiency to drop slightly. As the amount of

dextrose cryoprotectant increased, the labeling efficiency of the NP continued to decrease with the most drastic reduction from 0.01% dextrose to 0.1% dextrose. At the highest concentration of dextrose (5%), the labeling efficiency is at the lowest (~4%). The iron weight/cell and labeling efficiency for 5% sucrose is notably higher than that for 5% dextrose. With the exception of the noncryoprotected and 0.01% dextrose samples, all other NP samples had the similar labeling efficiencies as the benchmark Bangs microparticle, which has been previously demonstrated to robustly label STOs in 24 hours [11].

Discussion

Cryoprotection of polymer based nanoparticles is important during the fabrication process to enhance nanoparticle stability and assist in redispering in aqueous media [12]. Yet, while cryoprotection is clearly beneficial for inhibiting nanoparticle aggregation, there appear to be deleterious effects on magnetic cell labeling in culture. We found that noncryoprotected NPs labeled cells in culture more effectively than cryoprotected particles. Surprisingly, in this study comparing equivalent iron contents in the labeling media, noncryoprotected particles labeled cells even better than MPIOs.

The success of a particular particle to magnetically label cells is dependent on a number of factors. Cells have different mechanisms for internalizing nanoparticles – endocytosis, versus microparticles – phagocytosis [13;14]. Furthermore, for magnetic cell labeling in culture, particles need to settle to the bottom of the culture dish to interact with the cells. Smaller particles take longer to settle than larger particles. Additionally, particle surface charge influences the ability of particles to become internalized [15]. Lastly, hydrophobicity of particles plays a role in the ability of a particle to more rapidly associate with the hydrophobic lipids in the cell membrane, enhancing cellular uptake [16]. In this study, noncryoprotected particles are larger (aggregation), heavier (higher iron content by percent weight), more charged (sugars generally impart neutral charge) and more hydrophobic (PLGA is highly hydrophobic, sugars are hydrophilic); all of which enhancing magnetic cell labeling.

Because PLGA undergoes rapid hydrolysis in water, PLGA encapsulated iron oxide NPs require long term storage as a lyophilized powder. This study did not address the effect of cryoprotectant on nanoparticle stability and degradation rate. If indeed, cryoprotection has no effect on stability and degradation rate, than it is reasonable to suggest that cryoprotection of PLGA encapsulated iron oxide NPs fabricated for magnetic cell labeling is not necessary. If on the other hand, cryoprotection preserves nanoparticle stability and influences degradation rate, than some cryoprotection will likely be needed. It is important to note that one key finding in this study was that even though cryoprotected nanoparticles had reduced magnetic cell labeling efficiency compared to noncryoprotected particles, *all* of the different cryoprotected nanoparticles successfully labeled the fibroblasts at high levels of iron concentrations, well above the single cell detection limit on MRI (1 pg of iron/cell) [17;18]. Based on this study, the preliminary recommended cryoprotectant for MRI-based cell tracking would be 1% dextrose for a compromise between reduced particle aggregation and increased labeling efficiency. Different cell types and applications will affect this choice, e.g. short lived immune cells require higher labeling efficiency, and require more studies to

elucidate additional effects cryoprotection may have on cell labeling. Future work includes determining how long the redispersant effect lasts (how long the cryoprotectant prevents aggregation), how long the cryoprotectant associates with particles, and how well cryoprotected NPs label cells in an in vivo application.

Conclusion

The objective of this study was to identify a cryoprotection scheme to enhance redispersion of PLGA encapsulated iron oxide NPs in water and to study the effect this would have on magnetic cell labeling. We discovered that optimal percentage of dextrose for retaining initial particle characteristics was 1% with increasing percentages having little effect on average particle size and distribution and decreasing percentages having increasing degrees of aggregation. We found that for magnetic cell labeling, increasing dextrose cryoprotection decreased labeling efficiency, however all cryoprotectant percentages labeled cells robustly enough to enable single cell detection on MRI.

Reference List

1. Slotkin JR, Cahill KS, Tharin SA, Shapiro EM. Cellular magnetic resonance imaging: nanometer and micrometer size particles for noninvasive cell localization. Neurotherapeutics. 2007; 4(3):428–33. [PubMed: 17599708]
2. Nkansah MK, Thakral D, Shapiro EM. Magnetic poly(lactide-co-glycolide) and cellulose particles for MRI-based cell tracking. Magn Reson Med. 2011; 65(6):1776–85. [PubMed: 21404328]
3. De JF, Allemann E, Leroux JC, Stevels W, Feijen J, Doelker E, et al. Formulation and lyoprotection of poly(lactic acid-co-ethylene oxide) nanoparticles: influence on physical stability and in vitro cell uptake. Pharm Res. 1999; 16(6):859–66. [PubMed: 10397606]
4. Abdelwahed W, Degobert G, Stainmesse S, Fessi H. Freeze-drying of nanoparticles: formulation, process and storage considerations. Adv Drug Deliv Rev. 2006; 58(15):1688–713. [PubMed: 17118485]
5. Bozdag S, Dillen K, Vandervoort J, Ludwig A. The effect of freeze-drying with different cryoprotectants and gamma-irradiation sterilization on the characteristics of ciprofloxacin HCl-loaded poly(D,L-lactide-glycolide) nanoparticles. J Pharm Pharmacol. 2005; 57(6):699–707. [PubMed: 15969924]
6. Park J, An K, Hwang Y, Park JG, Noh HJ, Kim JY, et al. Ultra-large-scale syntheses of monodisperse nanocrystals. Nat Mater. 2004; 3(12):891–5. [PubMed: 15568032]
7. Chacon M, Molpeceres J, Berges L, Guzman M, Aberturas MR. Stability and freeze-drying of cyclosporine loaded poly(D,L lactide-glycolide) carriers. Eur J Pharm Sci. 1999; 8(2):99–107. [PubMed: 10210732]
8. Provencher SW. A Constrained Regularization Method for Inverting Data Represented by Linear Algebraic Or Integral-Equations. Computer Physics Communications. 1982; 27(3):213–27.
9. Hackley VA, Clogston JD. Measuring the hydrodynamic size of nanoparticles in aqueous media using batch-mode dynamic light scattering. Methods Mol Biol. 2011; 697:35–52. [PubMed: 21116952]
10. Konan YN, Gurny R, Allemann E. Preparation and characterization of sterile and freeze-dried sub-200 nm nanoparticles. International Journal of Pharmaceutics. 2002; 233(1–2):239–52. [PubMed: 11897428]
11. Tang KS, Shapiro EM. Enhanced magnetic cell labeling efficiency using -NH(2) coated MPIOs. Magn Reson Med. 2011; 65(6):1564–9. [PubMed: 21446031]
12. Hirsjarvi S, Peltonen L, Kainu L, Hirvonen J. Freeze-drying of low molecular weight poly(L-lactic acid) nanoparticles: effect of cryo- and lyoprotectants. J Nanosci Nanotechnol. 2006; 6(9–10): 3110–7. [PubMed: 17048525]

13. Ayhan H, Tuncel A, Bor N, Piskin E. Phagocytosis of monosize polystyrene-based microspheres having different size and surface properties. J Biomater Sci Polym Ed. 1995; 7(4):329–42. [PubMed: 7495763]

14. Piskin E, Tuncel A, Denizli A, Ayhan H. Monosize microbeads based on polystyrene and their modified forms for some selected medical and biological applications. J Biomater Sci Polym Ed. 1994; 5(5):451–71. [PubMed: 8038139]

15. Bennett KM, Zhou H, Sumner JP, Dodd SJ, Bouraoud N, Doi K, et al. MRI of the basement membrane using charged nanoparticles as contrast agents. Magn Reson Med. 2008; 60(3):564–74. [PubMed: 18727041]

16. Mulder WJ, Strijkers GJ, van Tilborg GA, Griffioen AW, Nicolay K. Lipid-based nanoparticles for contrast-enhanced MRI and molecular imaging. NMR Biomed. 2006; 19(1):142–64. [PubMed: 16450332]

17. Shapiro EM, Sharer K, Skrtic S, Koretsky AP. In vivo detection of single cells by MRI. Magn Reson Med. 2006; 55(2):242–9. [PubMed: 16416426]

18. Shapiro EM, Skrtic S, Sharer K, Hill JM, Dunbar CE, Koretsky AP. MRI detection of single particles for cellular imaging. Proc Natl Acad Sci U S A. 2004; 101(30):10901–6. [PubMed: 15256592]

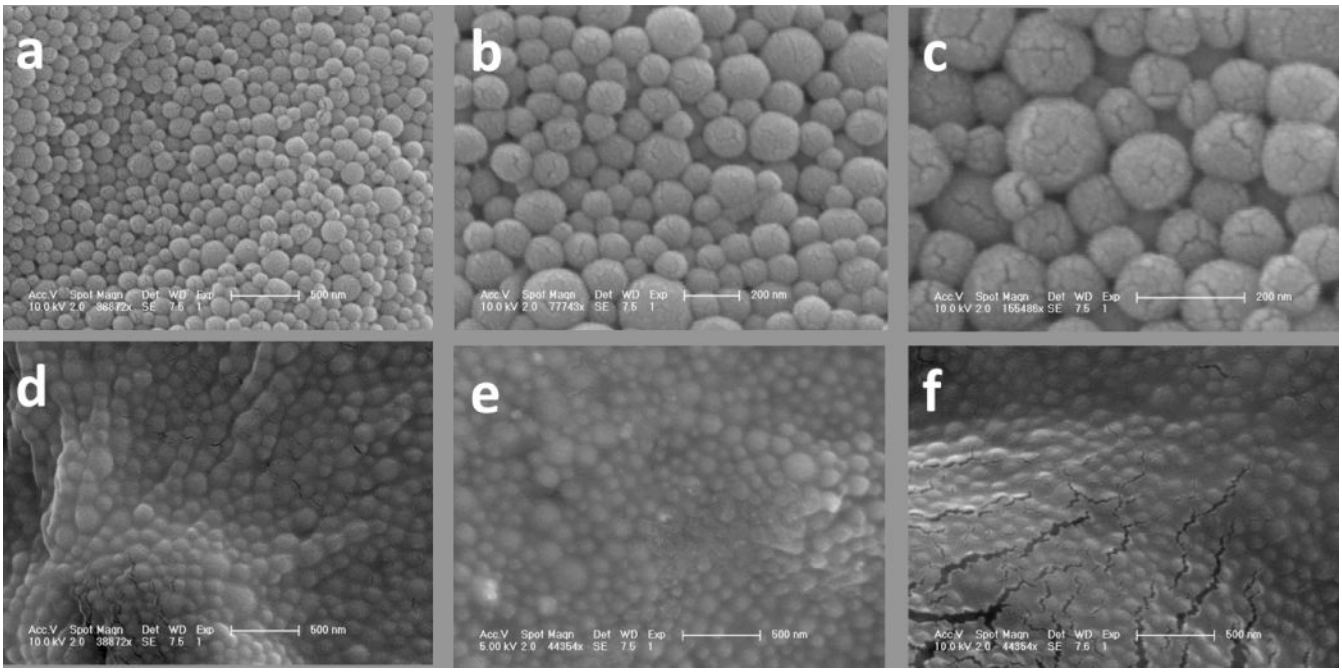

Figure 1.

SEM micrographs at different magnifications of magnetic PLGA encapsulated iron oxide NPs. (a)–(c) Noncryoprotected NPs freeze dried in pure DI water. Cracks seen are from the gold coating used for SEM visualization. (d) Cryoprotected NPs freeze dried in 2% dextrose, (e) 5% sucrose, and (f) 5% dextrose.

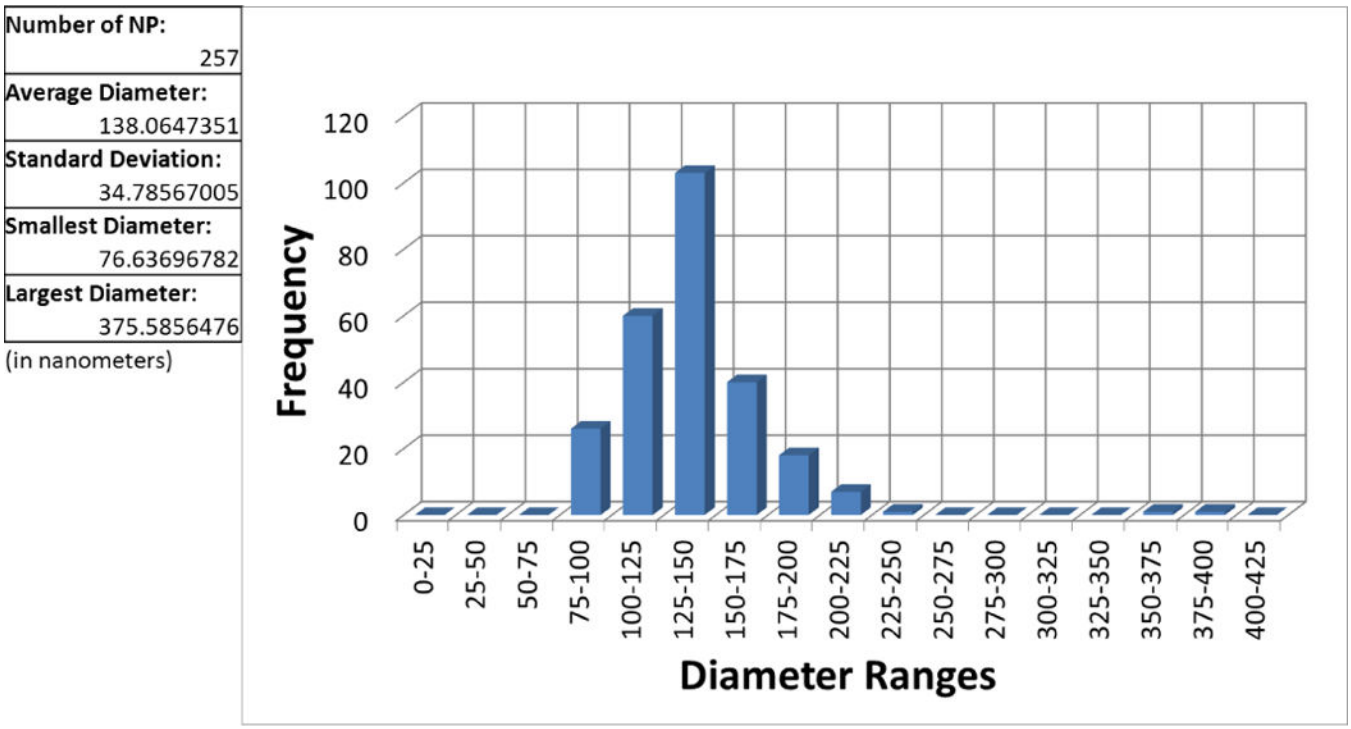

Figure 2.

Noncryoprotected nanoparticle size distribution. The 2D areas of 257 NPs on an SEM image were determined through ImageJ analysis and diameter of each NP calculated from the area of a circle.

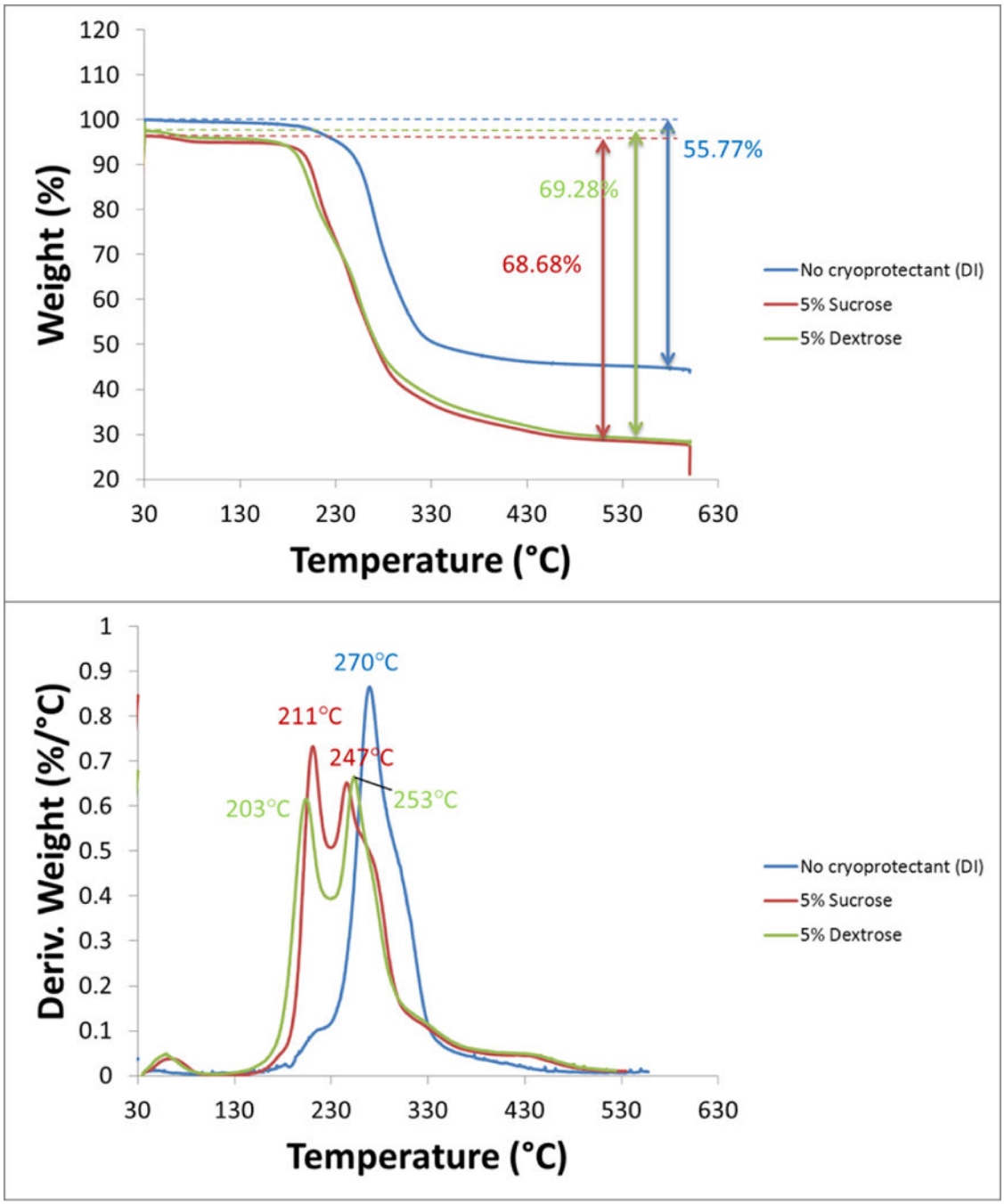

Figure 3.

TGA thermograms for PLGA encapsulated iron oxide NPs with no cryoprotectant (blue), 5% sucrose (red), 5% dextrose (green). The top graph plots the % weight as a function of temperature and shows the total percentage of PLGA polymer (and sugar if present) in the sample; the remaining weight at 600 °C is the magnetite. The bottom graph plots the magnitude of the weight % derivative as a function of temperature and highlights the temperature at which the PLGA polymer burns off. In the cryoprotected samples, there is an additional peak at ~200 °C highlighting the temperature at which the sugar burns off.

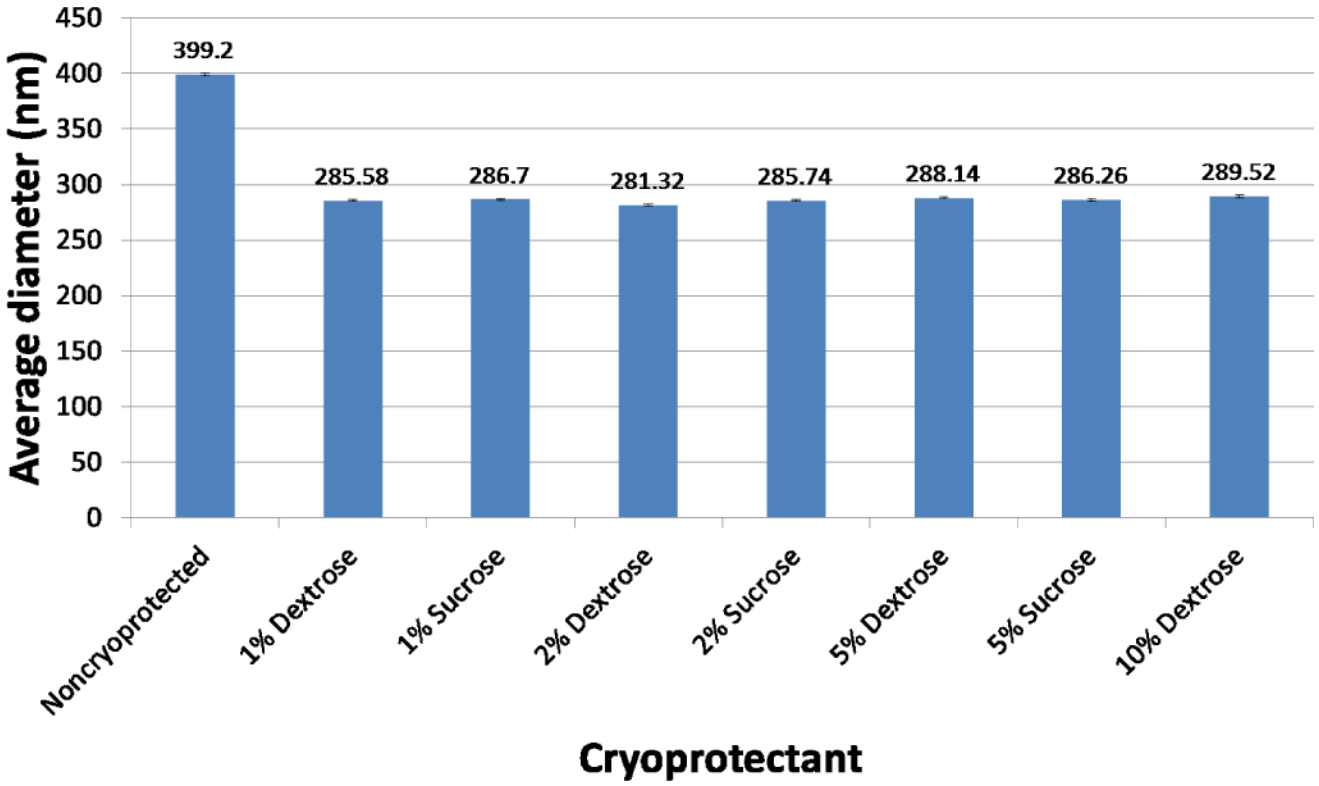

Figure 4.
Effect of cryoprotectant type and % on average NP size.

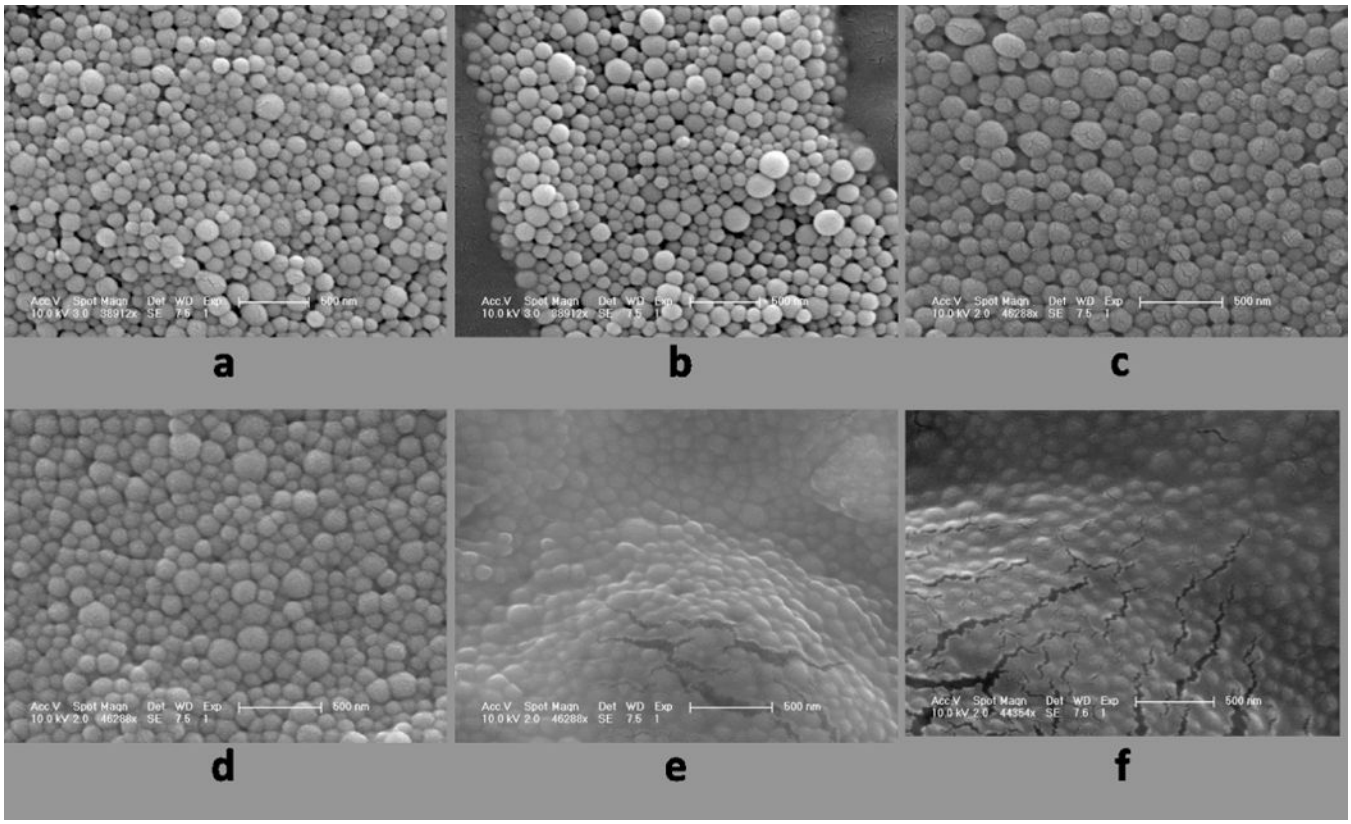

Figure 5.

SEM micrographs of PLGA encapsulated iron oxide NPs a) without cryoprotectant (freeze dried in DI water), b) 0.01% dextrose, c) 0.1% dextrose, d) 1% dextrose, e) 2% dextrose, and f) 5% dextrose. Sugar matrix is not visible until 2% dextrose.

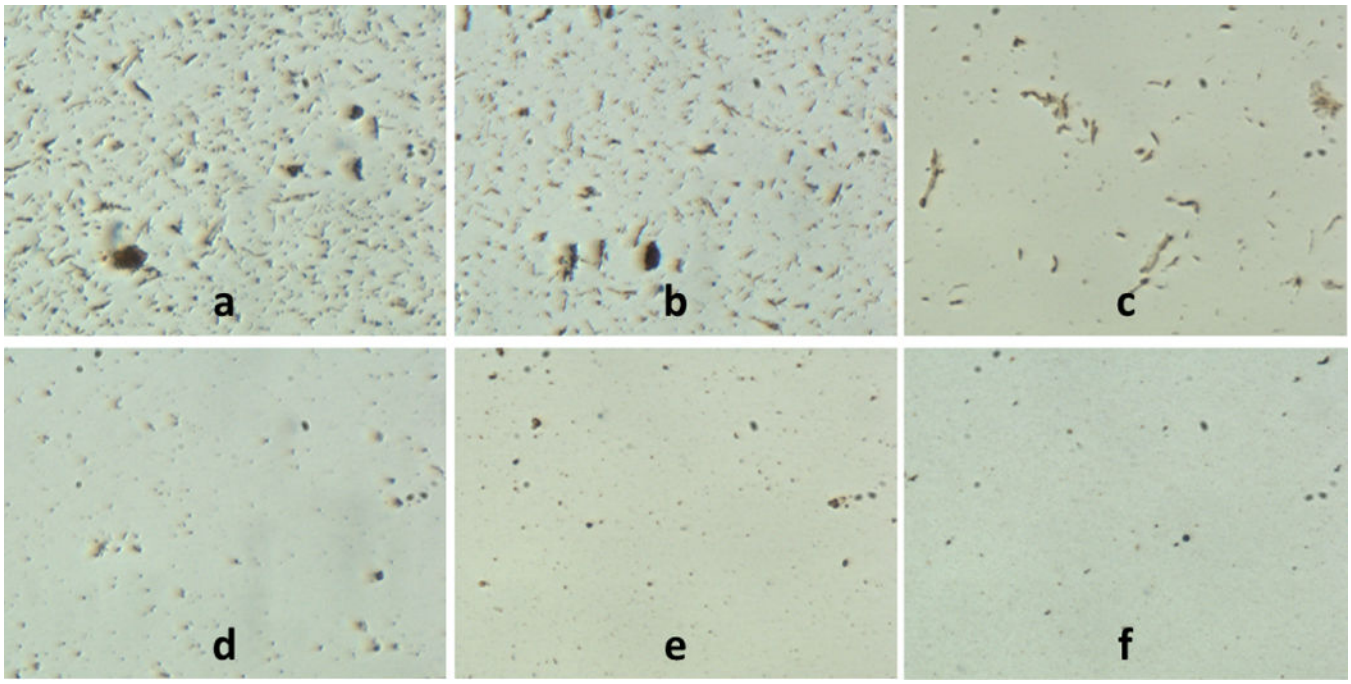

Figure 6.

Optical microscope images of a) noncryoprotected (DI) and cryoprotected (b–f) PLGA encapsulated iron oxide NPs in suspension. The amount of particle aggregation visibly decreases as cryoprotectant % increases: b) 0.01% dextrose, c) 0.1% dextrose, d) 1% dextrose, e) 2% dextrose, f) 5% dextrose

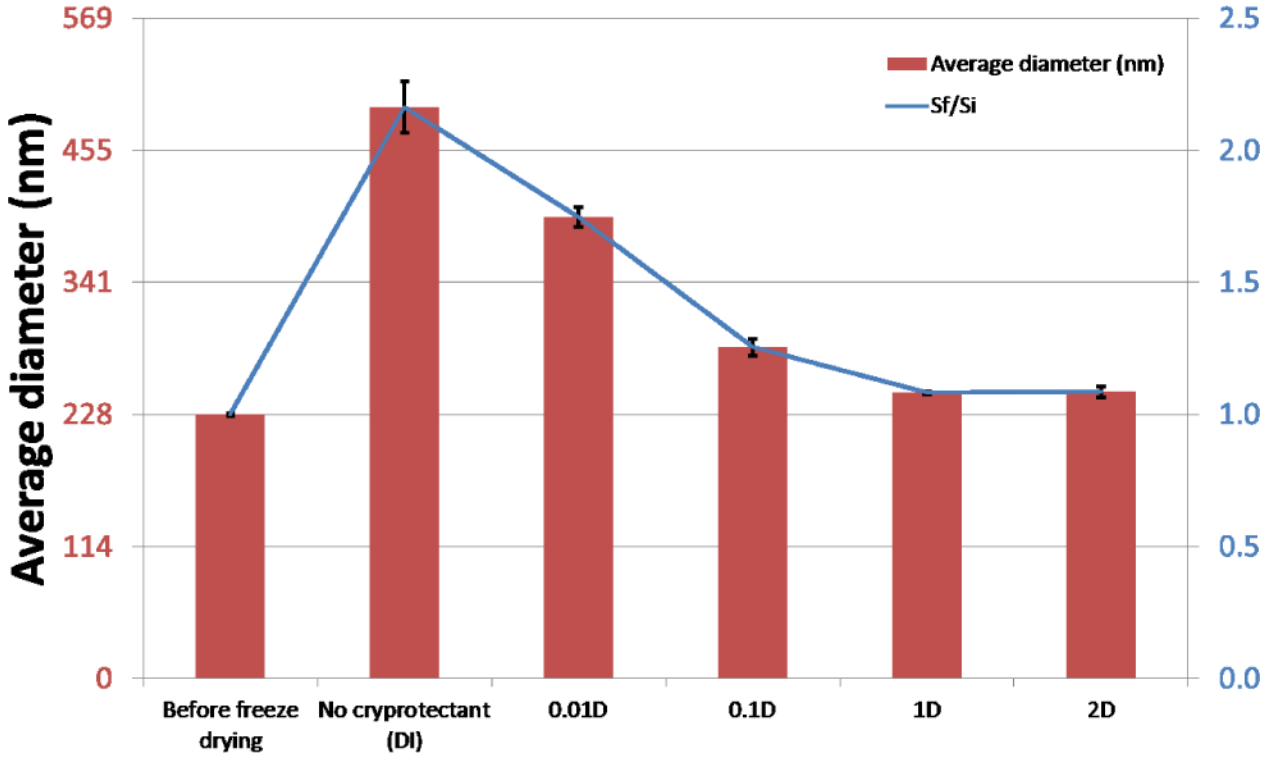

Figure 7.

Comparison charts of average particle sizes before freeze drying and after with and without cryoprotection. Top chart compares absolute average particle sizes. Bottom chart compares size ratios of particle size after freeze drying and initial particle size, S_f/S_i.

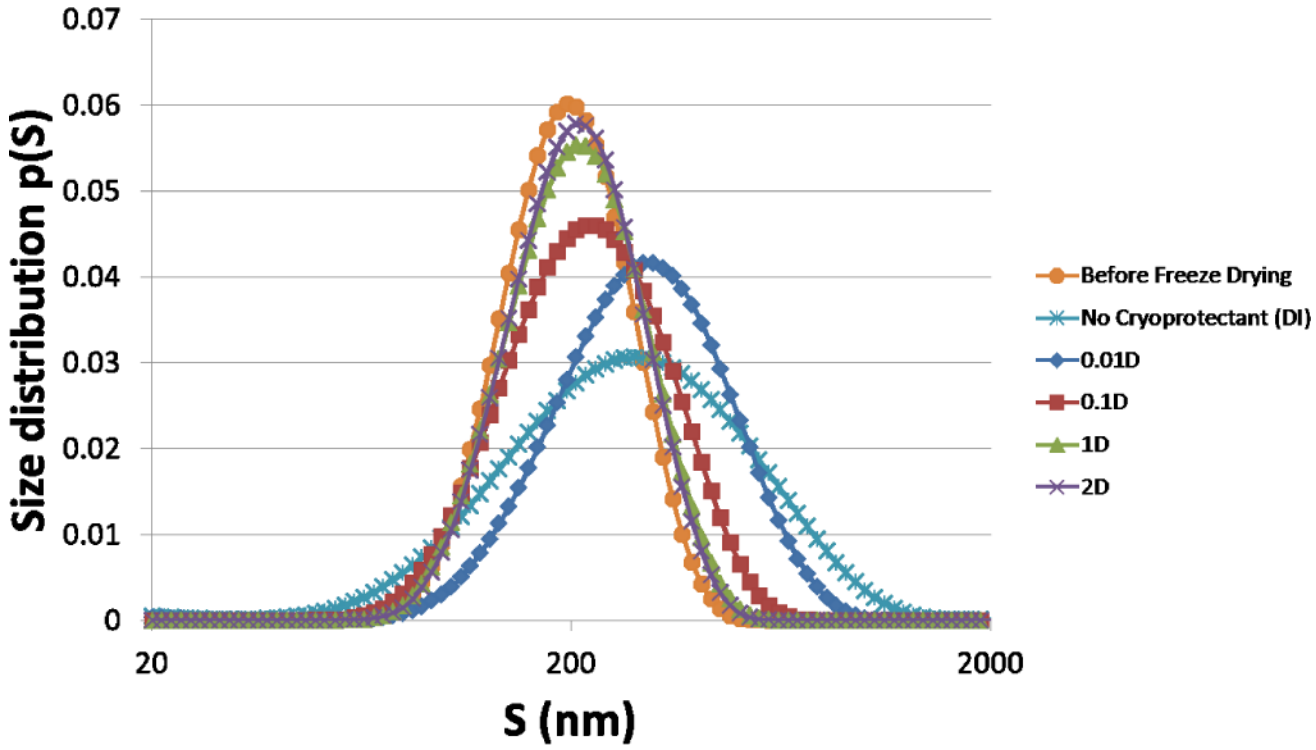

Figure 8.

Particle size distributions. CONTIN analysis of DLS data converted to size distributions p(S). The average size increase with decreasing amounts of cryoprotectant is accompanied by an increase in polydispersity of the particles in suspensions. X axis is in base 10 logarithmic scale.

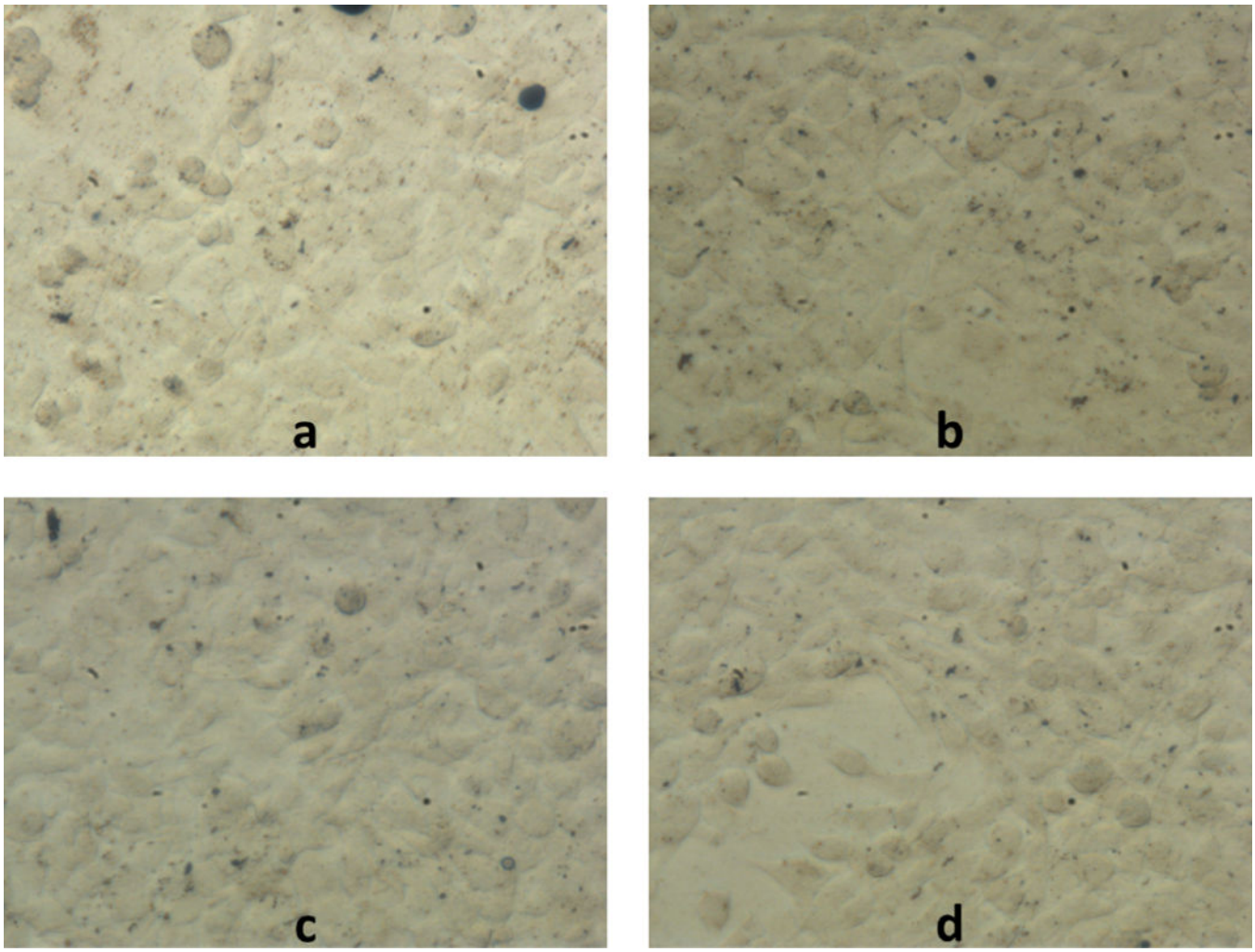

Figure 9.

Optical microscope images of STOs magnetically labeled with a) noncryoprotected NPs, b) 2% dextrose cryoprotected NPs, c) 5% sucrose cryoprotected NPs, and d) 5% dextrose cryoprotected NPs. Large aggregates of noncryoprotected NPs can be seen in the top left image of fibroblasts. Some 2% dextrose NP aggregates are visible in the top right and much less aggregation are visible in the 5% cryoprotectant samples. Scale bar = 50 microns.

Table 1

STO labeling doses for each particle and cryoprotectant type

Particle Type	Particle dose (mg/ml)	Iron dose (mg/ml)
No cryoprotectant	1.00	0.27
0.01% Dextrose (0.01D)	1.10	0.30
0.1% Dextrose (0.1D)	1.00	0.26
1% Dextrose (1D)	1.00	0.25
2% Dextrose (2D)	1.10	0.24
5% Dextrose (5D)	1.02	0.35
5% Sucrose (5S)	1.06	0.35
Bangs microparticle	0.94	0.31

Table 2

Summary of magnetic cell labeling experiment with different cryoprotectants

Sample	Iron/cell (pg/cell)	Labeling Efficiency (%)
No cryoprotectant	39.75	19.63
0.01% Dextrose	38.92	17.43
0.1% Dextrose	18.88	9.55
1% Dextrose	14.66	7.95
2% Dextrose	14.05	7.70
5% Dextrose	14.12	3.84
5% Sucrose	17.03	4.60
Bangs microparticle	20.22	6.10